*Research Article*

# Global Optimal Energy Management Strategy Research for a Plug-In Series-Parallel Hybrid Electric Bus by Using Dynamic Programming

**Hongwen He, Henglu Tang, and Ximing Wang**

*National Engineering Laboratory for Electric Vehicles, Beijing Institute of Technology, Beijing 100081, China*

Correspondence should be addressed to Hongwen He; hwhebit@bit.edu.cn

Energy management strategy influences the power performance and fuel economy of plug-in hybrid electric vehicles greatly. To explore the fuel-saving potential of a plug-in hybrid electric bus (PHEB), this paper searched the global optimal energy management strategy using dynamic programming (DP) algorithm. Firstly, the simplified backward model of the PHEB was built which is necessary for DP algorithm. Then the torque and speed of engine and the torque of motor were selected as the control variables, and the battery state of charge (SOC) was selected as the state variables. The DP solution procedure was listed, and the way was presented to find all possible control variables at every state of each stage in detail. Finally, the appropriate SOC increment is determined after quantizing the state variables, and then the optimal control of long driving distance of a specific driving cycle is replaced with the optimal control of one driving cycle, which reduces the computational time significantly and keeps the precision at the same time. The simulation results show that the fuel economy of the PEHB with the optimal energy management strategy is improved by 53.7% compared with that of the conventional bus, which can be a benchmark for the assessment of other control strategies.

## 1. Introduction

In recent years, the problems of energy shortage and environmental pollution have greatly promoted the development of electric vehicles (EVs). Among the EVs, the pure electric vehicles (PEVs) run with zero emissions and renewable electricity, but their disadvantages, such as the short operation range, high battery price, and long battery charging time, have limited the user's acceptability. The hybrid electric vehicles (HEVs) have longer operation range and higher performance than PEVs, but the electricity that keeps the battery state of charge (SOC) in a narrow window is still from the onboard fossil fuel [1, 2]. While the plug-in hybrid electric vehicle (PHEVs), with larger battery capacity, can run a long pure electric mileage and make full use of the cheap power from gird, hence it is more competitive than EVs and charge sustainable HEVs [3].

The energy management strategy is one of the key factors that influence the fuel economy and power performance of the PHEVs. In the PHEVs, in order to make full use of

the electricity energy stored in batteries, it is preferred that the battery energy drops to its minimum when the vehicle arrives at the destination. Therefore the energy management strategy becomes more complicated than that of the HEVs. Similar to HEVs, the energy management strategies in PHEVs can be usually classified into two categories: rule-based control strategies and optimization-based control strategies [4]. The main idea of rule-based control strategies is to make each component work in efficient area individually [5–7]. The reference [2] put forward a PHEV rule-based control strategy after considering the all-electric range and charge depletion range operations. The reference [5] proposed a PEHV rule-based energy management strategy by using the ADVISOR. The rule-based control strategies are simple and easy to implement, but they cannot safeguard the systematic optimization and cannot fully exploit the advantages of PHEVs.

The optimization-based control strategies include global optimization and real-time optimization. The real-time optimization realizes a local optimum step by step real timely

and loses the potential to get a global optimum. The adaptive control is a good example of real-time optimization, and the H$\infty$ control theory is powerful in adaptive control [8–11]. The global optimization finds an optimal solution for the whole process, which is suitable for energy management issues of the PHEB with regular driving cycle. For example, dynamic programming (DP) algorithm, which is effective to solve the constrained and nonlinear optimization problems, is selected to realize a global optimization of energy management for HEVs [12]. The reference [12] studied an optimal energy management of a parallel HEV with the known driving cycle using DP algorithm. The reference [13] built the driving cycle model using traffic information with the help of intelligent transportation systems and utilized the DP algorithm to study the global energy management optimization of a parallel plug-in hybrid electric sport utility vehicle (SUV). The reference [14] presented a way on how to implement the DP algorithm in the optimization of HEVs and carried out a global optimization with Toyota Prius as an example. The reference [15] determined an optimal energy management law for a two-clutch single-shaft parallel HEV by using optimization software, named KOALA. By comparisons, the DP algorithm has been proved to be powerful and effective in the global optimization of control strategies in HEVs. In this paper, a global optimization of the energy management strategy for a plug-in series-parallel hybrid bus (PHEB) is explored, and the battery energy state control is specially considered and discussed. The PHEB model was built in Section 2 and the global optimization problem with DP algorithm was put forward in Section 3. The DP numerical computation method was discussed and put forward in Section 4 and the simulation results were given in Section 5. Section 6 gives the main conclusions.

## 2. Plug-In Series-Parallel Hybrid Electric Bus Modeling

*2.1. Plug-In Series-Parallel Hybrid Electric Bus Configuration.* Figure 1 shows a schematic view of the PHEB powertrain, which includes a diesel engine, an integrated starter generator (ISG) motor, and a main drive motor. The ISG is connected to engine through a torsion damper. There is an on-off mode clutch between the ISG motor and the main drive motor. The PHEB works in parallel mode or engine-only mode when the mode clutch is in "ON" condition, and the diesel engine, ISG motor, and main drive motor drive the wheel mechanically. While the PHEB works in its series mode or all-electric mode when the mode clutch is in "OFF" condition, the main drive motor drives the wheels directly, and the diesel engine drives the ISG motor to generate electricity or not according to the battery state of charge. The main specific parameters of the PHEB are listed in Table 1.

*2.2. Plug-In Series-Parallel Hybrid Electric Bus Simulation Models.* There are two modeling methods in PHEV simulations. One is forward modeling, which is more accurate
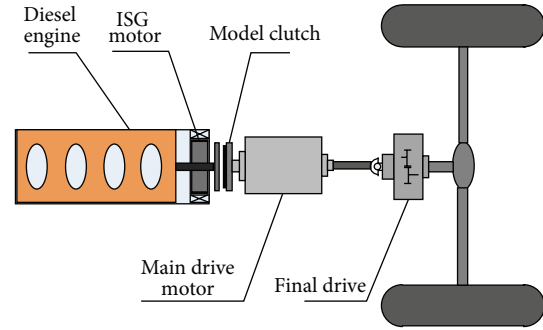


FIGURE 1: The plug-in series-parallel hybrid electric bus powertrain configuration.

TABLE 1: Main specific parameters of the plug-in series-parallel hybrid electric bus powertrain.

| Diesel engine | |
|---|---|
| Maximum power (kW) | 147 |
| Maximum torque (Nm) | 730 |
| ISG motor | |
| Maximum power (kW) | 55 |
| Maximum torque (Nm) | 500 |
| Drive motor | |
| Maximum power (kW) | 166 |
| Maximum torque (Nm) | 2080 |
| Battery | |
| Capacity (Ah) | 60 |
| Voltage (V) | 580 |
| Final drive ratio | 6.17 |
| Curb weight (kg) | 12500 |
| Gross weight (kg) | 18000 |
| Air resistance coefficient | 0.55 |
| Frontal area (m$^2$) | 6.6 |
| Tire dynamic radius (mm) | 473 |

but with heavier computational burden, and is always used to test the vehicle dynamic performance and drivability. The other one is the backward modeling, which is calculated with fixed time steps ignoring the dynamics of the powertrain components and usually is used to evaluate the vehicle fuel economy [16]. Since the global optimization is based on the fixed driving cycle and the DP problem is solved backward from the terminal of the driving cycle, we built the facing-backward simulation models as follows.

The diesel engine is modeled as a 3-dimension look-up table, where the inputs are the engine torque and speed and the output is the fuel consumption rate, as shown in Figure 2. The fuel consumption efficiency map is based on the experimental data.

The ISG motor is modeled as a 3-dimension look-up table based on the experimental efficiency map as shown in
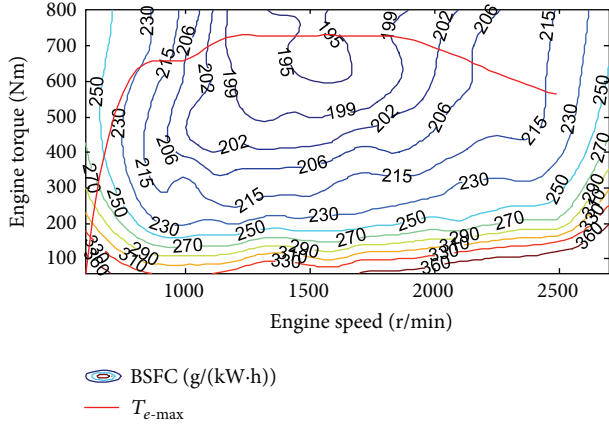
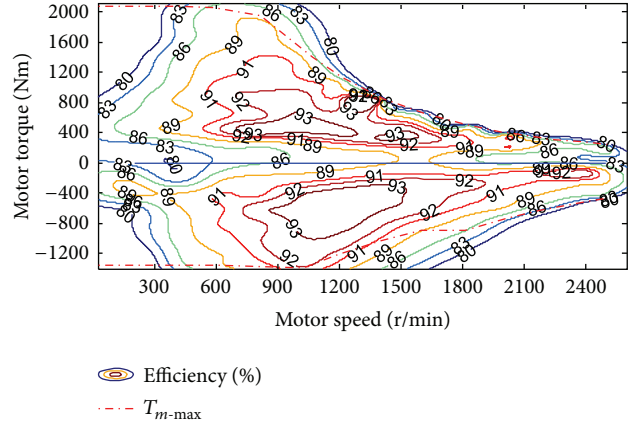FIGURE 2: The fuel consumption efficiency map of the diesel engine.



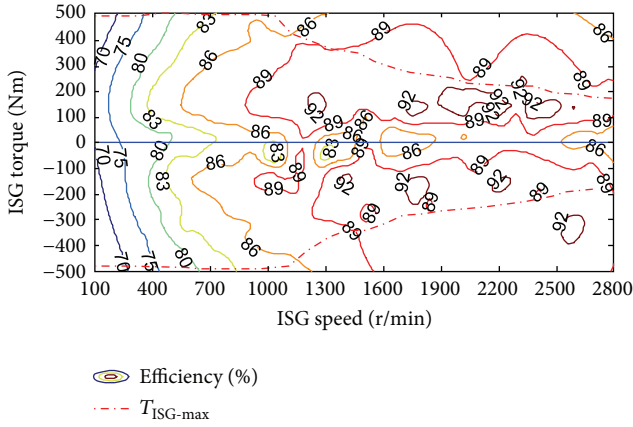FIGURE 4: The efficiency map of the main drive motor.



FIGURE 3: The ISG efficiency map.

Figure 3. Due to the limit of battery power, the output torque of ISG $T_{\text{ISG}}$ is described as follows:

$$
T_{\text{ISG}} =
\begin{cases}
\min\left(T_{\text{ISG\_req}}, T_{\text{ISG\_dis\_max}}(n_{\text{ISG}}),\right. \\
\quad\left. T_{\text{ISG\_bat\_dis\_max}}(n_{\text{ISG}}, \text{SOC})\right), & T_{\text{ISG\_req}} \geq 0 \\
\max\left(T_{\text{ISG\_req}}, T_{\text{ISG\_chg\_max}}(n_{\text{ISG}}),\right. \\
\quad\left. T_{\text{ISG\_bat\_chg\_max}}(n_{\text{ISG}}, \text{SOC})\right), & T_{\text{ISG\_req}} < 0,
\end{cases}
\tag{1}
$$

where $T_{\text{ISG\_req}}$ is the required ISG torque, $n_{\text{ISG}}$ is the ISG speed, SOC is the battery state of charge (SOC), $T_{\text{ISG\_dis\_max}}$ and $T_{\text{ISG\_chg\_max}}$ are the maximum ISG torque when driving and generating, respectively, and $T_{\text{ISG\_bat\_chg\_max}}$ and $T_{\text{ISG\_bat\_dis\_max}}$ are the torque limits due to battery current limits in the charging and discharging modes, which are functions of ISG speed and torque.

The main drive motor is modeled as a 3-dimension lookup table based on the experimental efficiency map as shown

in Figure 4. Due to the limit of battery power, the output torque of the main drive motor $T_m$ is as follows:

$$
T_m =
\begin{cases}
\min\left(T_{m\_req}, T_{m\_dis\_max}(n_m),\right. \\
\quad\left. T_{m\_bat\_dis\_max}(n_m, \text{SOC})\right) & T_{m\_req} \geq 0 \\
\max\left(T_{m\_req}, T_{m\_chg\_max}(n_m),\right. \\
\quad\left. T_{m\_bat\_chg\_max}(n_m, \text{SOC})\right), & T_{m\_req} < 0,
\end{cases}
\tag{2}
$$

where $T_{m\_req}$ is the required torque of the main drive motor, $n_m$ is the speed of the main drive motor, $T_{m\_dis\_max}$ and $T_{m\_chg\_max}$ are the maximum torque when driving and regenerative braking, respectively, and $T_{m\_bat\_chg\_max}$ and $T_{m\_bat\_dis\_max}$ are the torque limits due to battery current limits when charging and discharging, respectively, which are the functions of the main drive motor speed and torque.

The static equivalent circuit battery model described in [12] is used. The model inputs are the speed and torque of ISG and main drive motor, the model output is the battery SOC, which is calculated by (3)

$$
\begin{aligned}
\text{SOC}(k+1) = \text{SOC}(k) \\
- \left(V_{\text{oc}} - \left(V_{\text{oc}}^2 - 4(R_{\text{int}} + R_t)\right.\right. \\
\times \left(T_m \cdot n_m \cdot \eta_m^{-\text{sgn}(T_m)}\right. \\
\left.\left.\left. + T_{\text{ISG}} \cdot n_{\text{ISG}} \cdot \eta_{\text{ISG}}^{-\text{sgn}(T_{\text{ISG}})}\right)\right)^{1/2}\right) \\
\times \left(2(R_{\text{int}} + R_t) \cdot Q_b\right)^{-1},
\end{aligned}
\tag{3}
$$

where $R_{\text{int}}$ is the internal resistance, $V_{\text{oc}}$ is the open-circuit voltage, $R_{\text{int}}$ and $V_{\text{oc}}$ are the function of SOC, $Q_b$ is the maximum battery capacity, $R_t$ is the terminal resistance, $\eta_m$ and $\eta_{\text{ISG}}$ are the efficiencies of the main drive motor and ISG accordingly, and $k$ denotes the calculation step in discretization way.
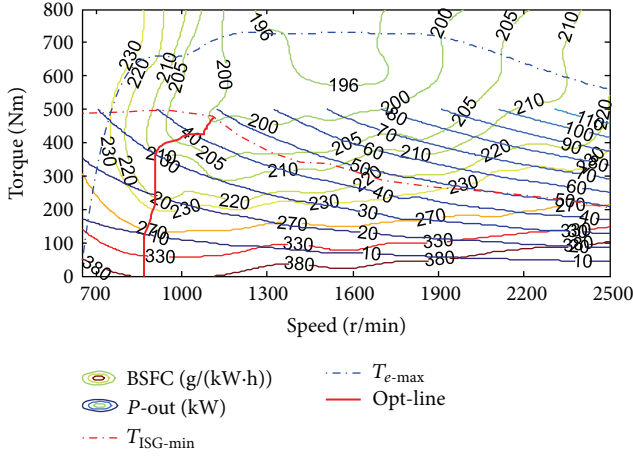
FIGURE 5: Engine-ISG fuel consumption map.

The mode clutch works in three conditions: disengaged, where clutch = 0; engaged, where clutch = 1; and half-engaged, where 0 < clutch < 1. The transition duration is very small, less than the time interval of the sample point of the driving cycle, so only two working conditions are considered in the dynamic optimization. If clutch = 1, the torque of engine and ISG motor can be delivered to final drive completely. If clutch = 0, only the main drive motor drives the vehicle.

When the PHEB works in series hybrid mode, taking the efficiency of engine and ISG into consideration, the minimum fuel consumption curve can be found as shown in Figure 5. For each required $P_{\text{ISG}}$, only the points on the minimum fuel consumption line are considered.

The time interval is set to 1 second. Assuming that the torques of the engine, main drive motor, and ISG remain constant in one time interval, we can calculate the vehicle dynamics as

$$
\begin{aligned}
v_v(k+1) &= v_v(k) \\
&+ \frac{1}{\delta M}\left(\frac{T_{\text{req}}(k)\cdot i_o\cdot\eta}{r_d}\right. \\
&\left.- \frac{v_v(k)}{|v_v(k)|}\left(F_f + F_a\left(v_v(k)\right)\right)\right),
\end{aligned}
\tag{4}
$$

where $T_{\text{req}}$ is the total required torque as the input of the final drive, $\eta$ is the mechanical powertrain efficiency, $i_o$ is the final drive ratio, $v_v$ is the vehicle speed, $r_d$ is the dynamic tire radius, $\delta M$ is the effective mass of the vehicle, and $F_a$ and $F_f$ are aerodynamic drag force and rolling resistance force, respectively.

According to (4), we can get the $T_{\text{req}}$ as the driving cycle is known in advance. For the PHEB powertrain, the relationship between $T_{\text{req}}$ and the powertrain components can be expressed as

$$
T_{\text{req}}(k) = T_e(k) + T_{\text{ISG}}(k) + T_m(k) + \frac{T_b(k)}{i_o},
\tag{5}
$$

where $T_b$ is the hydraulic brake torque and $T_e$ is the engine torque.

## 3. Global Optimal Energy Management Strategy Modeling

For PHEB, DP aims to find the control of each stage to minimize the cost function over the whole driving cycles. The control variables and state variables are determined before DP problem is formulated. The state variables, including vehicle speed $v_v$ and SOC, reflect the operating state of the system. As the driving cycle and the vehicle speed $v_v$ in every stage are known, SOC is chosen as the state variable. There are many control variables in the PHEB such as engine torque $T_e$, engine speed $n_e$, motor torque $T_m$, ISG torque $T_{\text{ISG}}$, and hydraulic brake torque $T_b$, but only three of them are independent. Here the $n_e$, $T_e$, and $T_m$ are chosen as the independent control variables.

In the discrete-time format, the PHEB system can be expressed as

$$
x(k+1) = f(x(k), u(k)),
\tag{6}
$$

where $x(k)$ and $u(k)$ are state vector and control vector, respectively.

For PHEB, the price of electricity is very low compared with that of diesel when used to drive the same distance [13], so we focus our research on minimizing the fuel consumption. The cost function is built as follows:

$$
J = \sum_{k=0}^{N-1} L(x(k), u(k)) = \sum_{k=0}^{N-1} \text{fuel}(k),
\tag{7}
$$

where $N$ is the duration of the driving cycle, and $L$ is the instantaneous cost; fuel denotes the diesel consumption.

If the SOC drops below the lower limit, the battery will not supply electricity to the main drive motor. To avoid the condition that the engine cannot supply the required torque, another cost function should be considered besides (7) then the cost function rewrites as follows:

$$
\begin{aligned}
J &= \sum_{k=0}^{N-1} L(x(k), u(k)) \\
&= \sum_{k=0}^{N-1}\left[\text{fuel}(k) + \alpha\left(T_{\text{req}}(k) - T_e(k)\right.\right. \\
&\left.\left. - T_{\text{ISG}}(k) - T_m(k) - \frac{T_b(k)}{i_o}\right)^2\right],
\end{aligned}
\tag{8}
$$

where $\alpha$ is a positive weighting factor.

Constrains (5) and (9) are necessary to ensure a smooth operation of the engine, ISG, main drive motor, and batteries

during the optimization. Consider

$$n_{e\text{-min}} \leq n_e(k) \leq n_{e\text{-max}},$$

$$T_{e\text{-min}}(n_e(k)) \leq T_e(k) \leq T_{e\text{-max}}(n_e(k)),$$

$$T_{\text{ISG-min}}(n_{\text{ISG}}(k), \text{SOC}(k)) \leq T_{\text{ISG}}(k)$$
$$\leq T_{\text{ISG-max}}(n_{\text{ISG}}(k), \text{SOC}(k)),$$

$$T_{m\text{-min}}(n_m(k), \text{SOC}(k)) \leq T_m(k)$$
$$\leq T_{m\text{-max}}(n_m(k), \text{SOC}(k)),$$

$$\text{SOC}_{\min} \leq \text{SOC}(k) \leq \text{SOC}_{\max},$$

$$n_m(k) = n_e(k) = n_{\text{ISG}}(k) \quad \text{if clutch} = 1,$$

$$n_e(k) = n_{\text{ISG}}(k) \quad \text{if clutch} = 0,$$

$$T_e(k) + T_{\text{ISG}}(k) = 0 \quad \text{if clutch} = 0.$$

$$(9)$$

## 4. A Numerical Computation for the DP Problem

Based on Bellman's Principle of Optimization, the global optimization problem can be solved by dealing with a sequence of subproblems of optimization backward from the terminal of the driving cycle [17, 18]. Then the DP problem can be described by the recursive equation (10)-(11). The subproblem for $(N-1)$ step is

$$J_{N-1}^*(x(N-1)) = \min_{u(N-1)} [L(x(N-1), u(N-1))]. \quad (10)$$

For step $k$ $(0 \leq k < N - 1)$, the subproblem is

$$J_k^*(x(k)) = \min_{u(k)} [L(x(k), u(k)) + J_{k+1}^*(x(k+1))], \quad (11)$$

where $J_k^*(x(k))$ is the optimal cost-to-go function at state $x(k)$ from stage $k$ to the end of the driving cycle and $x(k+1)$ is the state in stage $k+1$ after the control $u(k)$ is applied to state $x(k)$ at stage $k$ according to (6).

*4.1. Solving the DP Problem Backward.* The recursive equation (10)-(11) is solved backward, and quantization and interpolation are needed to solve the equation. The continuous state SOC is discretized into finite grids first, and the number of discretized state $S$ is

$$S = \frac{(\text{SOC}_{\max} - \text{SOC}_{\min})}{\delta\text{SOC}}, \quad (12)$$

where $\delta\text{SOC}$ is the increment of the discretized SOC and $\text{SOC}_{\max}$ and $\text{SOC}_{\min}$ are upper and lower constrains of SOC.

Then find all possible control solutions at every state of each stage. The function $J_k^*(x(k))$ at every grid points of SOC is evaluated, and $J_{k+1}^*(x(k+1))$ is evaluated by interpolation if the calculated value of admissible $\text{SOC}_{k+1}$ in (3) does not fall exactly on grid points. The way of interpolation is shown in [13]. The procedure of solving the DP problem backward
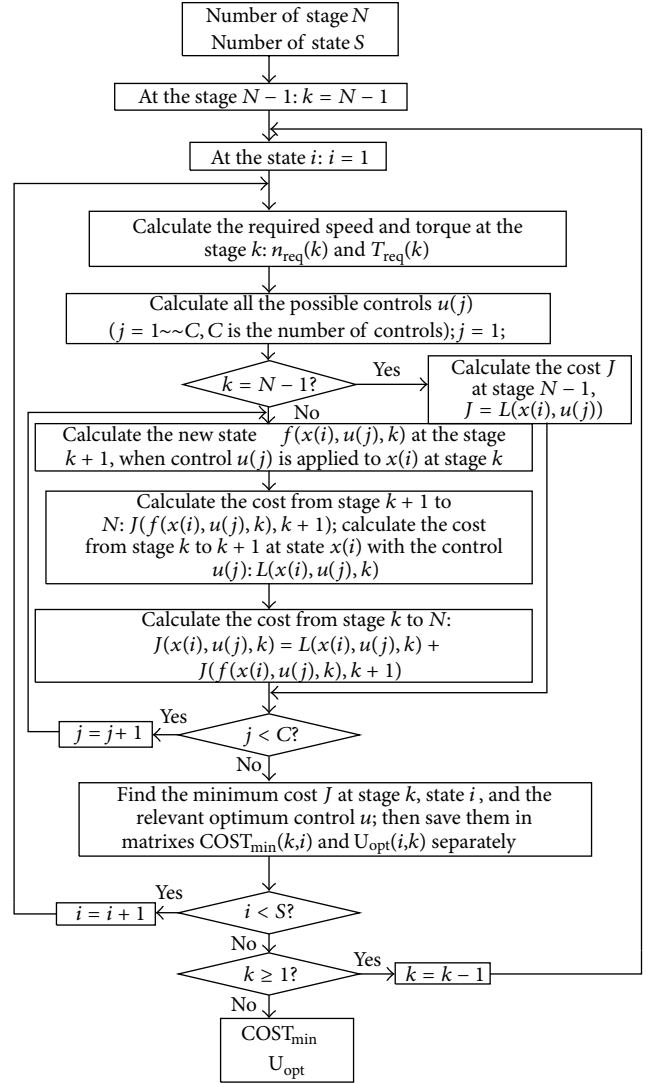


Figure 6: The flow chart of solving the DP problem backward.

is shown in Figure 6, where the required speed $n_{\text{req}}$ is the same as driving cycle and required torque is determined by inversely solving vehicle dynamic model as shown in (4).

*4.1.1. To Find All Possible Control Solutions.* It is very important to find all possible control solutions in the procedure of solving the DP problems backward. The possible control solutions are the possible combination of the discrete torque of the components in each state of the driving cycle which meets the torque need of the vehicle. The number of the control solutions influences the accuracy of the optimization greatly, and the way to search for all the control solutions influences the computational burden significantly. To get a compromise, here we find the possible working modes of the PHEB first, and then we find all possible control solutions in every mode; finally we get all the control solutions at every grid point of SOC.

The PHEB works in many modes, such as engine-only mode, battery electric (EV) mode, engine-ISG parallel mode,
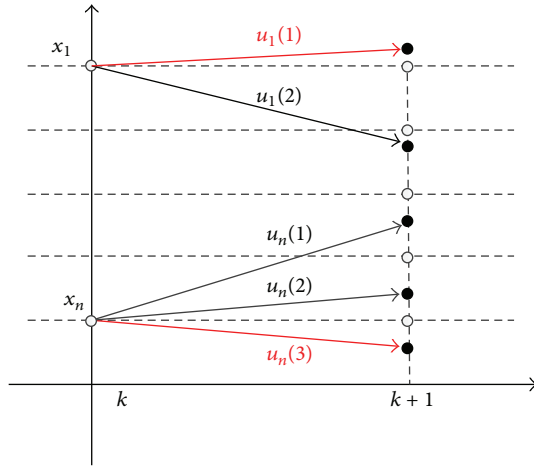
FIGURE 7: Schematic diagram of state transformation with control variables.



FIGURE 8: The required speed and torque of the final drive when $SOC < SOC_{low}$.



FIGURE 9: The required speed and torque of final drive when $SOC_{low} < SOC < SOC_{high}$.

engine-motor parallel mode, and series mode. The ISG is used as a starter and generator and will not drive the bus directly. Only when the torque required by the vehicle exceeds the maximum torque that can be provided by the main drive motor and engine together, the ISG will provide the remaining torque.

According to (6), the state variables in the $x(k + 1)$ may exceed the range of SOC, as shown in Figure 7, where the state at stage $k + 1$ exceeds the range of SOC with the control variables $u_1(1)$ and $u_n(3)$. To avoid this situation, the control variables should be limited. We divide SOC into three areas: $SOC_{max} \geq SOC \geq SOC_{high}$, $SOC_{min} \leq SOC \leq SOC_{low}$, and $SOC_{low} < SOC < SOC_{high}$. The initial SOC and terminal SOC are usually in the area $SOC_{low} < SOC < SOC_{high}$.

(A) When the SOC is higher than high limit $SOC_{high}$, the motor drives the bus without regenerative braking. Only when the torque required by the vehicle exceeds the maximum torque that can be provided by drive motor, ISG will supply positive torque to drive the bus. If more driving power is required, the engine comes to work to supply the remaining torque.

(B) When the SOC drops below the low limit $SOC_{low}$, the battery will not supply electric energy any more. According to the required torque and required speed areas of final drive shown in Figure 8, the PHEB works in different modes as listed in Table 2. The blue line in Figure 8 represents the maximum output torque of the motor with the power supplied by engine, ISG, when PHEB works in series mode.

(C) If $SOC_{low} < SOC < SOC_{high}$, the torque that can be supplied by the powertrain components is shown in Figure 9. The possible working modes are shown in Table 3.

If the PHEB works in series mode, discretize the minimum fuel consumption curve into finite points, and the engine/ISG works on these points. If the PHEB works in engine-motor parallel mode, such as the PHEV which works
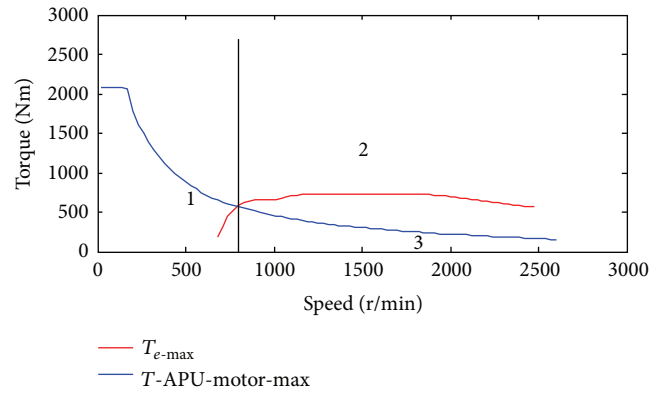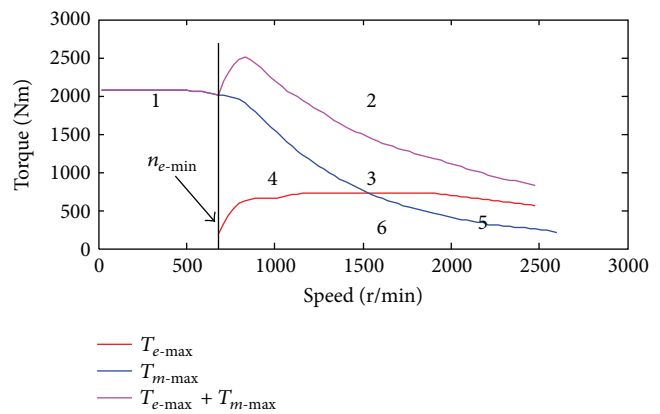
on area 3 in Figure 9, the flow chart to find all possible controls is shown in Figure 10(a). If the PHEB works in the same mode on areas 4, 5, and 6 in Figure 9, the initial condition of $T_e$ is set to be $T_{req}$. If the PHEB works in engine-ISG parallel mode, the way to find the possible controls is shown in Figure 10(b).

*4.2. To Find the Optimal Control Path Forward.* The optimal controls at every state point of every stage are obtained by solving the DP problem backward; if the initial SOC is specified, the optimal control path will be found forward. The interpolation is also needed to find the optimal control path as shown in Figure 11. If the optimal control at stage $k$ is $u_k$, the optimal control $u_{k+1}$ at stage $k + 1$ is got through interpolation between the controls $u_{k+1}(i)$ and $u_{k+1}(i + 1)$, which are the optimal controls at state grid points $x(i)$ and $x(i + 1)$, respectively, at stage $k + 1$.

## 5. Simulation Results

For the PHEB, it is reasonable to make full use of the battery energy. Considering the health and the efficiency of the battery, the low level, the high level, and the initial SOCs were
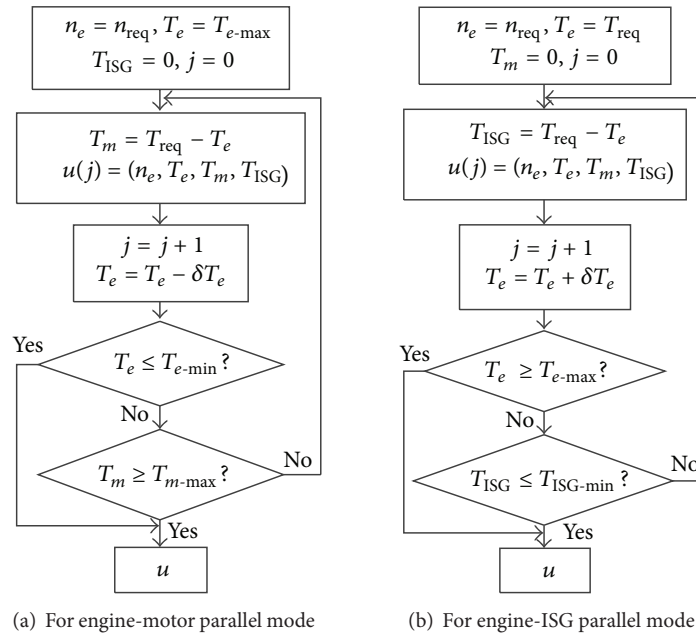
(a) For engine-motor parallel mode   (b) For engine-ISG parallel mode

FIGURE 10: The way to find possible control solutions.

TABLE 2: Working modes when SOC < SOC$_{low}$.

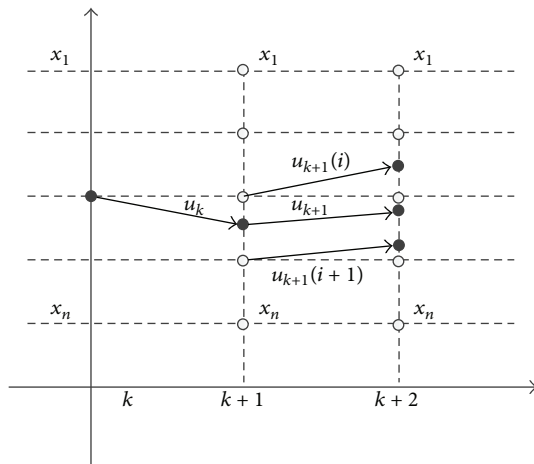| The required speed and torque areas of the final drive in Figure 8 | PHEB possible working mode | Remarks |
| --- | --- | --- |
| 1 | Series mode | Engine/ISG works in maximum power point |
| 2 | Engine-only mode | Engine only drives the PHEB |
| 3 | Engine-ISG parallel mode | Engine drives the PHEB, and the ISG generates as much electric energy as possible to charge the battery |



FIGURE 11: The schematic diagram of interpolation.
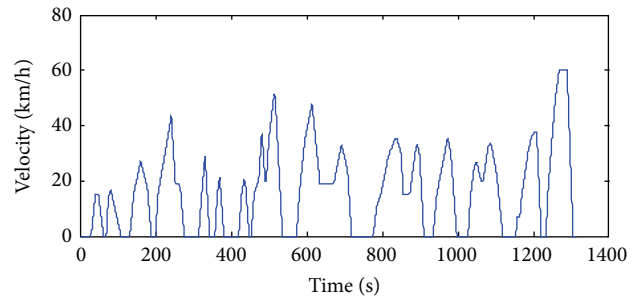


FIGURE 12: The profile for one CTUDC driving cycle.

selected to be 0.3, 0.8, and 0.6, respectively. The driving cycle is the Chinese typical urban drive cycle (CTUDC) as shown in Figure 12. The total distance of one CTUDC is 5.897 km, and the duration of one CTUDC is 1314 seconds.

The battery capacity of PHEB is much higher than that of HEVs, and the PHEB drives with the mode of one day

one charge, so the PHEB would drive for many consecutive driving cycles. To show the energy distribution between the engine, ISG, and main drive motor, the model is simulated with the input of 15 consecutive CTUDC cycles. The increment of discretized SOC, $\delta$SOC, is selected to be 0.001, the increment of engine torque $\delta T_e$ is selected to be 5 Nm, the weighting factor $\alpha$ is selected to be 100, and the PHEB weight of simulation is set to be the gross weight.

Figure 13 shows the simulation result of SOC under the DP optimal control for 15 consecutive CTUDC cycles.

TABLE 3: Possible PHEB modes when $SOC_{low} < SOC < SOC_{high}$.

| Required torque and speed areas of final drive | PHEB possible working modes | Remarks |
|---|---|---|
| 1 | EV mode, series mode | If the motor cannot supply sufficient torque, the ISG motor will provide the remaining torque |
| 2 | Engine-ISG-motor parallel mode | The required torque of final drive exceeds the maximum torque provided by engine and motor together, and ISG motor provides remaining torque |
| 3 | Engine-motor parallel mode | None |
| 4 | EV mode, series mode, engine-motor parallel mode | None |
| 5 | engine-ISG parallel mode, engine-motor parallel mode, engine-only mode | None |
| 6 | Engine-only mode, EV mode, engine-ISG parallel mode, engine-motor parallel mode, series mode | None |
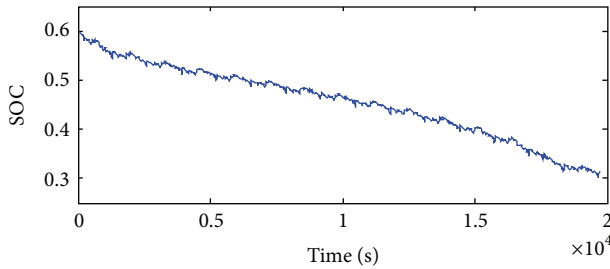


FIGURE 13: The SOC simulation result for 15 CTUDC cycles.



Simulation result
CTUDC

FIGURE 14: Velocity comparison between simulation and CTUDC cycle.

The SOC decreased to 0.314 when the bus reached the destination. Because of the regenerative braking at the end of the cycle, the terminal SOC is a little higher than the low level, but it is still very close to the low level, so the bus can make full use of the battery energy with the optimal control.

The SOC decreases evenly from the initial SOC to the low level of the SOC. When the optimal control was applied to the 15 consecutive CTUDC cycles, the SOC reduction would be 0.02 for one cycle on average. To relieve the heavy computational burden, the optimal control for one CTUDC cycle can be used as the optimal control for 15 consecutive CTUDC driving cycles through restricting the initial SOC and terminal SOC. The initial SOC and desired terminal SOC are selected to be 0.5 and 0.48, respectively. To ensure that the SOC at final time is the desired value, an additional terminal constrain on SOC needs to be imposed and the cost function would be

$$
\begin{aligned}
J &= \sum_{k=0}^{N-1} L(x(k), u(k)) \\
&= \sum_{k=0}^{N-1} \left[ \text{fuel}(k) + \alpha \left( T_{\text{req}}(k) - T_e(k) - T_{\text{ISG}}(k) \right.\right. \\
&\qquad\qquad \left.\left. - T_m(k) - \frac{T_b(k)}{i_o} \right)^2 \right] \\
&\quad + \beta \left( \text{SOC}(N) - \text{SOC}_f \right)^2,
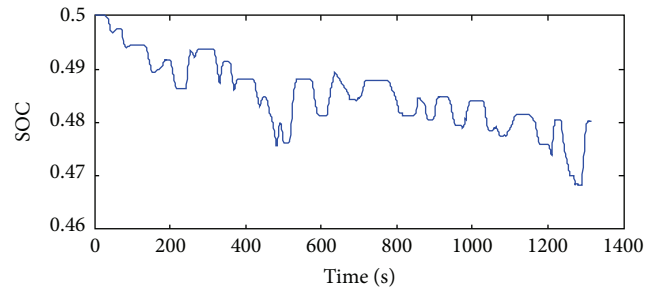\end{aligned}
$$

(13)



FIGURE 15: The SOC simulation result for one CTUDC cycle.

where $\beta$ is positive weighting factor and $SOC_f$ is the desired SOC at the end of driving cycle.

The increment of SOC, $\delta SOC$, is selected to be 0.001, the increment of engine torque $\delta T_e$ is selected to be 5 Nm, and the weighting factors $\alpha$ and $\beta$ are selected to be 100 and $1 \times 10^7$, respectively. The difference between simulation result of velocity and desired vehicle velocity is very small as shown in Figure 14. Figure 15 shows the simulation result of SOC with the optimal control for one driving cycle, and the terminal SOC turned out to be 0.4804, which is very close to the desired value.

TABLE 4: The simulation results for different driving cycles.

| Number of driving cycle | 15 | 1 |
|---|---|---|
| Distance (km) | 88.46 | 5.897 |
| Initial SOC | 0.6 | 0.5 |
| Terminal SOC | 0.314 | 0.4804 |
| Electric energy consumption (kWh) | 9.95 | 0.682 |
| Fuel consumption (L) | 17.44 | 1.174 |
| Fuel consumption per 100 km (L/100 km) | 19.72 | 19.90 |
| Computation time (s) | 50220.8 | 2643.2 |

The simulation results for 15 consecutive driving cycles and one driving cycle are shown in Table 4. The fuel consumption per 100 km of 15 driving cycles is 19.72 L, and the fuel consumption per 100 km of one driving cycle with restricted terminal SOC is 19.90 L. The fuel consumption per 100 km increased by 0.91%, while the computation time decreased by 94.7%. Considering that the internal resistance of the battery is a function of SOC, the optimal control of one driving cycle with restricted terminal SOC is applied to the simulation for 15 consecutive driving cycles, and the simulation result is shown in Table 5.

With the optimal control for one driving cycle, the fuel consumption per 100 km increased by 0.91% and the electric energy consumption increased by 3.2%, but the terminal SOC is still higher than the low level. The computation time of solving DP problem to find the optimal control decreased significantly, so it is feasible to find the optimal controls for consecutive driving cycles by solving the DP problem for one driving cycle with restricted initial SOC and terminal SOC.

The state increment $\delta$SOC in (12) also influences the accuracy of the optimization. If the $\delta$SOC is smaller, the quantized search area will be larger, hence the computational burden will be heavier. To study the tradeoff between accuracy of the optimization and computation time, $\delta$SOC is selected to be 0.0005, 0.001, and 0.005, respectively. The SOC simulation results are shown in Figure 16. The terminal SOC dropped to 0.4802, 0.4804, and 0.4806, respectively, which are very close to the desired value. When $\delta$SOC is selected to be 0.001, the curve of SOC is very similar to the curve when $\delta$SOC is selected to be 0.0005.

The fuel consumption and computation time results are summarized in Table 6. Compared with the results when $\delta$SOC is 0.0005, the fuel consumption increased by 0.61% and the computation time decreased by 53.9% when $\delta$SOC is 0.001, while the fuel consumption increased by 7.03% and the computation time decreased by 91.0% when $\delta$SOC is 0.005. Considering the tradeoff between fuel consumption and computation time, it is feasible to set $\delta$SOC to be 0.001. And the simulation results in this case are shown in Figure 17.

The output torque of the PHEB components is shown in Figure 17. It can be seen that the ISG seldom works as a generator to charge the battery, and most of the negative power is from regenerative braking. If the ISG works as a generator, there are engine efficiency losses, ISG efficiency losses, main drive motor efficiency losses, and battery efficiency losses, hence the system is ineffective, so in most cases the optimal
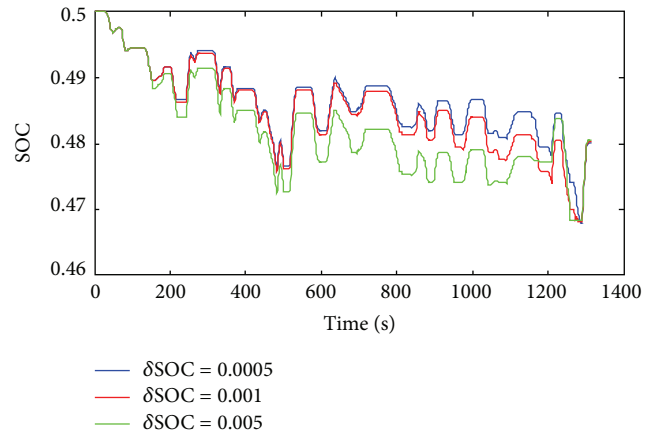


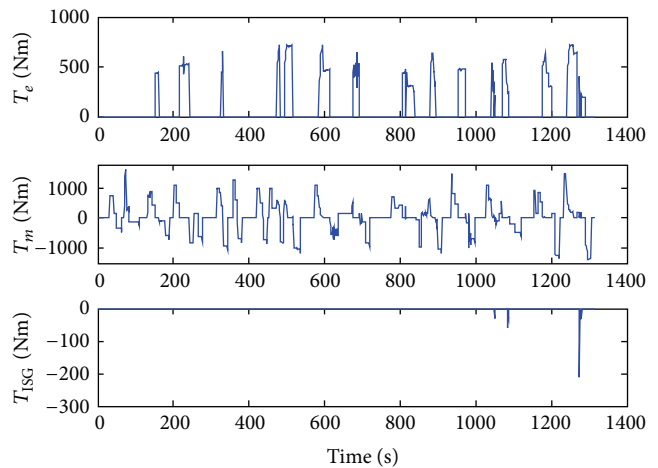FIGURE 16: The SOC simulation results with different $\delta$SOCs.



FIGURE 17: The simulation results with DP optimal control when $\delta$SOC is 0.001.
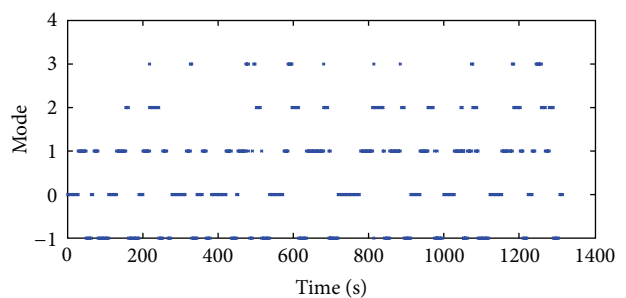


FIGURE 18: The PHEB working modes under optimal control strategy.

control strategy based on DP avoids the situation when the ISG works as a generator. At the end of the cycle, to force the terminal SOC to be the desired value, the ISG supplied negative power to charge the battery.

The working modes of the PHEB is shown in Figure 18, where mode = 0 means that the bus stops and no powertrain components is working; mode = −1 means regenerative
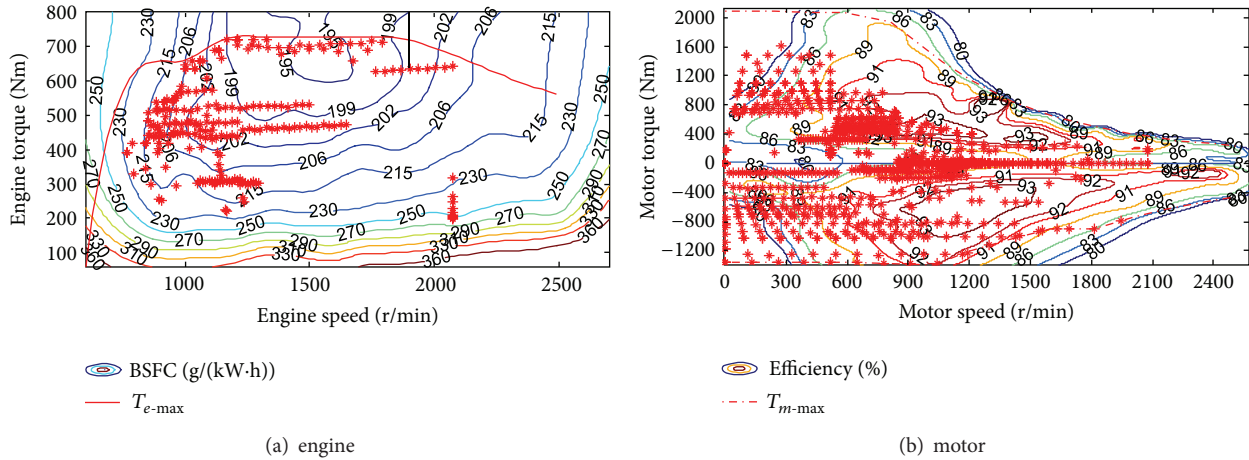
(a) engine



(b) motor

FIGURE 19: Working areas of the components.

TABLE 5: Simulation results for different control strategies.

| Control strategy | Number of driving cycle | Initial SOC | Terminal SOC | Electric energy consumption (kWh) | Fuel consumption (L) | Fuel consumption per 100 km (L/100 km) |
|---|---|---|---|---|---|---|
| DP optimal control for 15 consecutive cycles | 15 | 0.6 | 0.314 | 9.95 | 17.44 | 19.72 |
| DP optimal control for one cycle with restricted initial and terminal SOCs | 15 | 0.6 | 0.305 | 10.27 | 17.603 | 19.90 |

TABLE 6: Simulation result of fuel consumption and computation time.

| $\delta$SOC | 0.0005 | 0.001 | 0.005 |
|---|---|---|---|
| Fuel consumption per 100 km (L/100 km) | 19.78 | 19.90 | 21.17 |
| Computation time (s) | 5733.4 | 2643.2 | 517.4 |

braking mode, mode = 1 means EV mode, mode = 2 means engine-only mode, mode = 3 means parallel mode, and mode = 4 means series mode. It can be seen that the system does not work in series mode in case of the low efficiency.

When the PHEB works in full load condition and the load rate of engine is high, the engine can work in high efficiency area without need of the load regulation of ISG, so the ISG seldom supplies negative torque. The working points of engine and main drive motor are shown in Figure 19. It shows that the engine works in high efficiency areas in most cases. The main drive motor drives the bus alone when the vehicle speed is low. The engine works if the vehicle required speed is high and the main drive motor supplies the remaining torque to maintain the engine working in high efficiency. The ISG seldom works under the optimal control based on DP, but it does not mean that the ISG is useless, because the energy control strategy of the PHEB is based on rules in reality, the driving distance is not a fixed value, and the ISG is needed to charge the battery to maintain the SOC level. There is

no standard PHEB fuel consumption for rule-based energy management control strategy, and the PHEB may consume more fuel than traditional bus if the control rule parameters were not properly designed. So we made a comparison of the fuel consumption between the PHEB with optimized control strategy and the prototype conventional diesel bus. The results show that the experimented fuel consumption of the prototype conventional diesel bus is 43 L/100 km in CTUDC driving cycle, and the fuel consumption of the optimized PHEB is 19.90 L/100 km, with additional electricity consumption of 11.61 kWh/100 km, the fuel consumption decreased by 53.7%. The optimal control based on DP can improve fuel economy significantly. It should be noted that the fuel consumption results given by the optimal control based on DP are maximum potential gains, and they cannot be reached in a real vehicle, because the entire driving cycle is known in advance, and neither comfort constraints nor highly dynamic phenomena are taken into account [15].

## 6. Conclusions

It is very complicated to determine the energy management strategy for a series-parallel PHEB, and the dynamic programming is a powerful tool to get global optimization results. The backward simulation model of the series-parallel PHEB was built. Then, to explore the potential of fuel economy, the dynamic programming algorithm is utilized to

realize an optimal control on a known-in-advance driving cycle. The procedure of DP for the series-parallel powertrain topology is introduced in detail. An appropriate method is proposed to improve the computational efficiency which can reduce the computation burden greatly and keep the precision of DP.

The simulation results show that with the global optimal control, the battery SOC can reach its lower limit at the end of the cycle, which means that the bus can make full of the battery energy. Meanwhile, the ISG seldom works in generation mode under given cycle and SOC interval, which avoids the inefficient situation. It is proved that the optimal control based on DP can reduce the fuel consumption greatly.

The drawback of optimal control based on DP is that the driving cycle should be known in advance, and the computational burden is still very heavy, so it is difficult to be applied in a real vehicle. In the further study, a near-optimal control law will be extracted according to the global optimization results.

## Conflict of Interests

The authors declare that there is no conflict of interests regarding the publication of this paper.

## Acknowledgments

## References

[1] M. Ehsani, Y. Gao, and A. Emadi, *Modern Electric, Hybrid Electric, and Fuel Cell Vehicles: Fundamentals, Theory, and Design*, CRC Press, New York, NY, USA, 2009.

[2] Y. Gao and M. Ehsani, "Design and control methodology of plug-in hybrid electric vehicles," *IEEE Transactions on Industrial Electronics*, vol. 57, no. 2, pp. 633–640, 2010.

[3] C. H. Stephan and J. Sullivan, "Environmental and energy implications of plug-in hybrid-electric vehicles," *Environmental Science and Technology*, vol. 42, no. 4, pp. 1185–1190, 2008.

[4] S. G. Wirasingha and A. Emadi, "Classification and review of control strategies for plug-in hybrid electric vehicles," *IEEE Transactions on Vehicular Technology*, vol. 60, no. 1, pp. 111–122, 2011.

[5] H. Banvait, S. Anwar, and Y. Chen, "A rule-based energy management strategy for plugin hybrid electric vehicle (PHEV)," in *Proceedings of the American Control Conference (ACC '09)*, pp. 3938–3943, St. Louis, Mo, USA, June 2009.

[6] N. J. Schouten, M. A. Salman, and N. A. Kheir, "Fuzzy logic control for parallel hybrid vehicles," *IEEE Transactions on Control Systems Technology*, vol. 10, no. 3, pp. 460–468, 2002.

[7] P. Pisu and G. Rizzoni, "A comparative study of supervisory control strategies for hybrid electric vehicles," *IEEE Transactions on Control Systems Technology*, vol. 15, no. 3, pp. 506–518, 2007.

[8] H. Zhang, Y. Shi, and M. Liu, "$H_\infty$ step tracking control for networked discrete-time nonlinear systems with integral and predictive actions," *IEEE Transactions on Industrial Informatics*, vol. 9, no. 1, pp. 337–345, 2013.

[9] H. Zhang, Y. Shi, and A. S. Mehr, "Robust $H_\infty$ PID control for multivariable networked control systems with disturbance/noise attenuation," *International Journal of Robust and Nonlinear Control*, vol. 22, no. 2, pp. 183–204, 2012.

[10] H. Zhang, Y. Shi, and A. S. Mehr, "Robust weighted $H_\infty$ filtering for networked systems with intermittent measurements of multiple sensors," *International Journal of Adaptive Control and Signal Processing*, vol. 25, no. 4, pp. 313–330, 2011.

[11] H. Zhang, Y. Shi, and A. S. Mehr, "Robust static output feedback control and remote PID design for networked motor systems," *IEEE Transactions on Industrial Electronics*, vol. 58, no. 12, pp. 5396–5405, 2011.

[12] C.-C. Lin, H. Peng, J. W. Grizzle, and J.-M. Kang, "Power management strategy for a parallel hybrid electric truck," *IEEE Transactions on Control Systems Technology*, vol. 11, no. 6, pp. 839–849, 2003.

[13] Q. Gong, Y. Li, and Z.-R. Peng, "Trip-based optimal power management of plug-in hybrid electric vehicles," *IEEE Transactions on Vehicular Technology*, vol. 57, no. 6, pp. 3393–3401, 2008.

[14] W. Wang and S. M. Lukic, "Dynamic programming technique in hybrid electric vehicle optimization," in *Proceedings of the IEEE International Electric Vehicle Conference*, pp. 4–8, Greenville, SC, USA, March 2012.

[15] J. Scordia, M. Desbois-Renaudin, R. Trigui, B. Jeanneret, F. Badin, and C. Plasse, "Global optimisation of energy management laws in hybrid vehicles using dynamic programming," *International Journal of Vehicle Design*, vol. 39, no. 4, pp. 349–367, 2005.

[16] W. Zheng, *Reseach on power train parameter matching method and control strategy for hybrid electric vehicle [Ph.D. thesis]*, Harbin Institute of Technology, Harbin, China, 2010.

[17] Y. Zou, S. J. Hou, and E. L. Han, "Dynamic programming-based energy management strategy optimization for hybrid electric commercial vehicle," *Automotive Engineering*, vol. 34, no. 8, pp. 663–668, 2012.

[18] R. Bellman, *Dynamic Programming*, Princeton University Press, Princeton, NJ, USA, 1957.

Advances in
Operations Research

Advances in
Decision Sciences

Journal of
Applied Mathematics

Algebra

Journal of
Probability and Statistics

The Scientific
World Journal

International Journal of
Differential Equations

International Journal of
Combinatorics

# Hindawi

Submit your manuscripts at
http://www.hindawi.com

Advances in
Mathematical Physics

Journal of
Complex Analysis

Journal of
Mathematics

Mathematical Problems
in Engineering

Abstract and
Applied Analysis

Discrete Dynamics in
Nature and Society

International
Journal of
Mathematics and
Mathematical
Sciences

Journal of
Discrete Mathematics

Journal of
Function Spaces

International Journal of
Stochastic Analysis

Journal of
Optimization